# Supplementary Information

Open-space Microfluidics as a Tool to Study Notch Signaling Dynamics

Maude Proulx,[a] Pierre Clapperton-Richard, [a] Laurent Potvin-Trottier,[b] Alisa Piekny[b] and Thomas Gervais*[c,d,e]

# I. Device design and parameters optimization

3 criteria were considered to design the device:

1. Transition time between reagent switching must be low.
2. Shear stress must be limited under 1 Pa as much as possible to keep cells viable.
3. Confinement zones' (petals) area must be high enough to cover at least 100 cells.

To fit these criteria, scaling laws for the microfluidic dipole described by Safavieh et al., (2015) were considered.[1] If conformal mapping applied to obtain a rotational (flower) configuration might affect flow geometry[2], they are useful here to estimate the parameters' vicinities.

1. Transition time

An important value to consider is the Péclet number to assess the diffusive or convective nature of the transport. Near the MFP stagnation point (where velocity is zero), Péclet was described as[1]:

$$P\acute{e} = \frac{Q_{inj}\,(\alpha - 1)^3}{8\pi G D \alpha}$$

With D being the diffusion coefficient of the diluted specie. The characteristic time $t_0$ for the diffusion profile to reach its permanent regime of the MFP was described as:

$$t_0 = \frac{r^2}{4DP\acute{e}}$$

Where r is the distance between the injection and aspiration aperture (or petal radius). Thus, a longer petal radius might lead to a greater transition time, while high Péclet numbers will reduce it.

2. Shear stress

The shear stress for a Hele-Shaw flow was described as[1]:

$$\tau(x, y) = \frac{6\eta}{G}\vec{v}(x, y)$$

Where $\eta$ is the fluid viscosity and $\vec{v}(x, y)$ is the velocity. The height of the gap G is thus inversely proportional to the shear stress.

3. Confinement zones' area

The confinement zones' area varies with the petal radius and $\alpha$, which dictates the petal's width (Fig S1). The area necessary to expose 100 cells of 40 µm at 50% confluence was estimated at 0.4 mm$^2$. Hence, at least 0.4 mm$^2$ of the petal area must be kept under the set value of 1 Pa.

Taking these factors into account, the parameters G, $\alpha$, $Q_{inj}$, and $r$ were chosen to maximize petal area, minimize transition time and minimize the shear stress. Final values are presented in Table S1. With these values, Reynolds numbers were also calculated ($Re = \frac{\rho v L}{\eta}$, with $L = \frac{G^2}{r}$) for a microfluidic dipole (Safavieh et al., 2015). Reynolds numbers for the whole velocity field are shown in Fig S2.

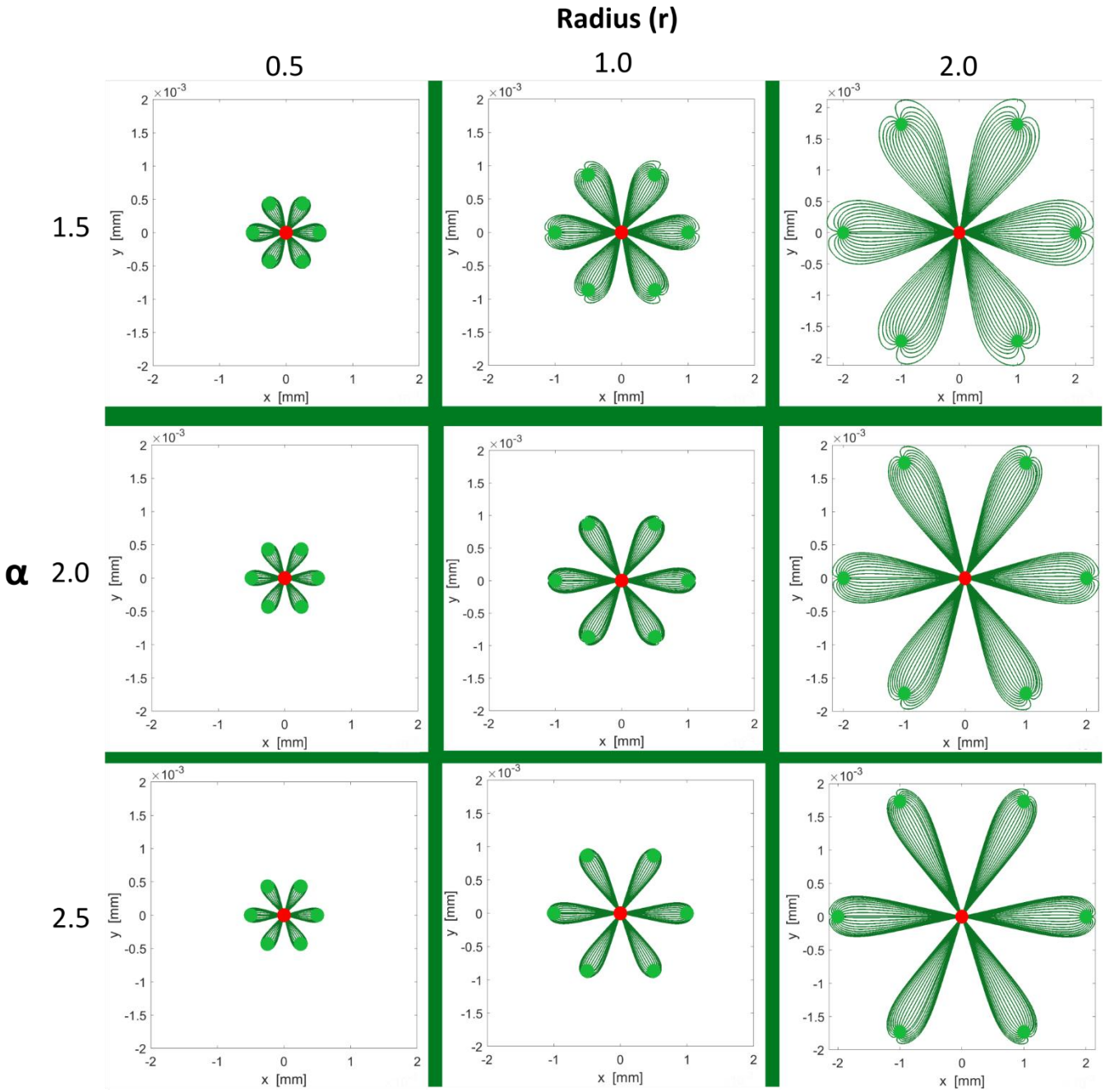


*Fig S1 - The petals' area varies according to the α ratio, which dictates width, and radius R, which dictates lengths.*

*Table S1. Design and operation parameters of the microfluidic display for Notch dynamics experiments.*

| Parameter | Value |
|---|---|
| $\alpha$ | 1.3 |
| $Q_{inj}$ | 0.4 $\mu L/s$ |
| $r$ | 1.15 $mm$ |
| $G$ | 100 $\mu m$ |

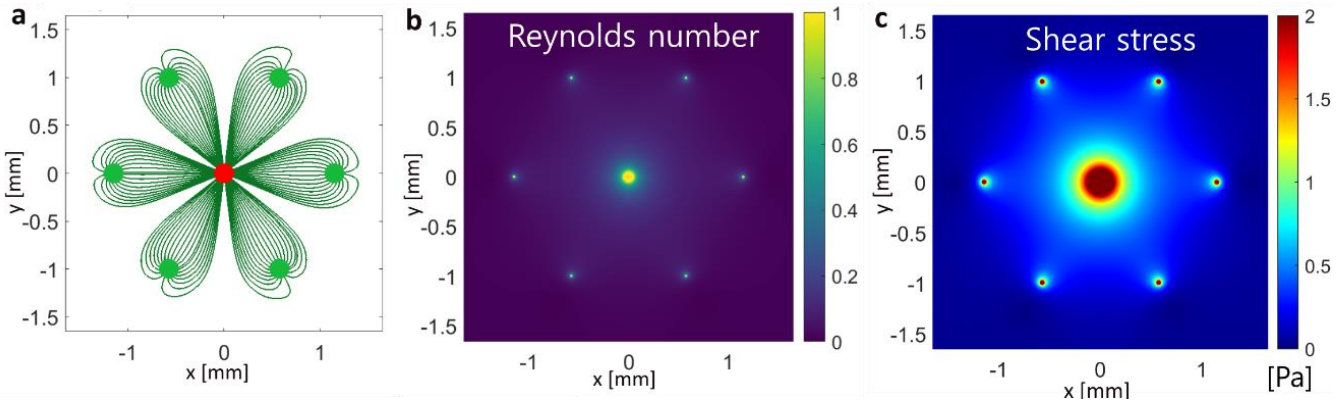


*Fig S2– Theoretical flow characterization of the configuration with the final design and operation parameters. (a) Streamlines, (b) Reynolds number and (c) Shear stress.*

# II. Reagent delivery

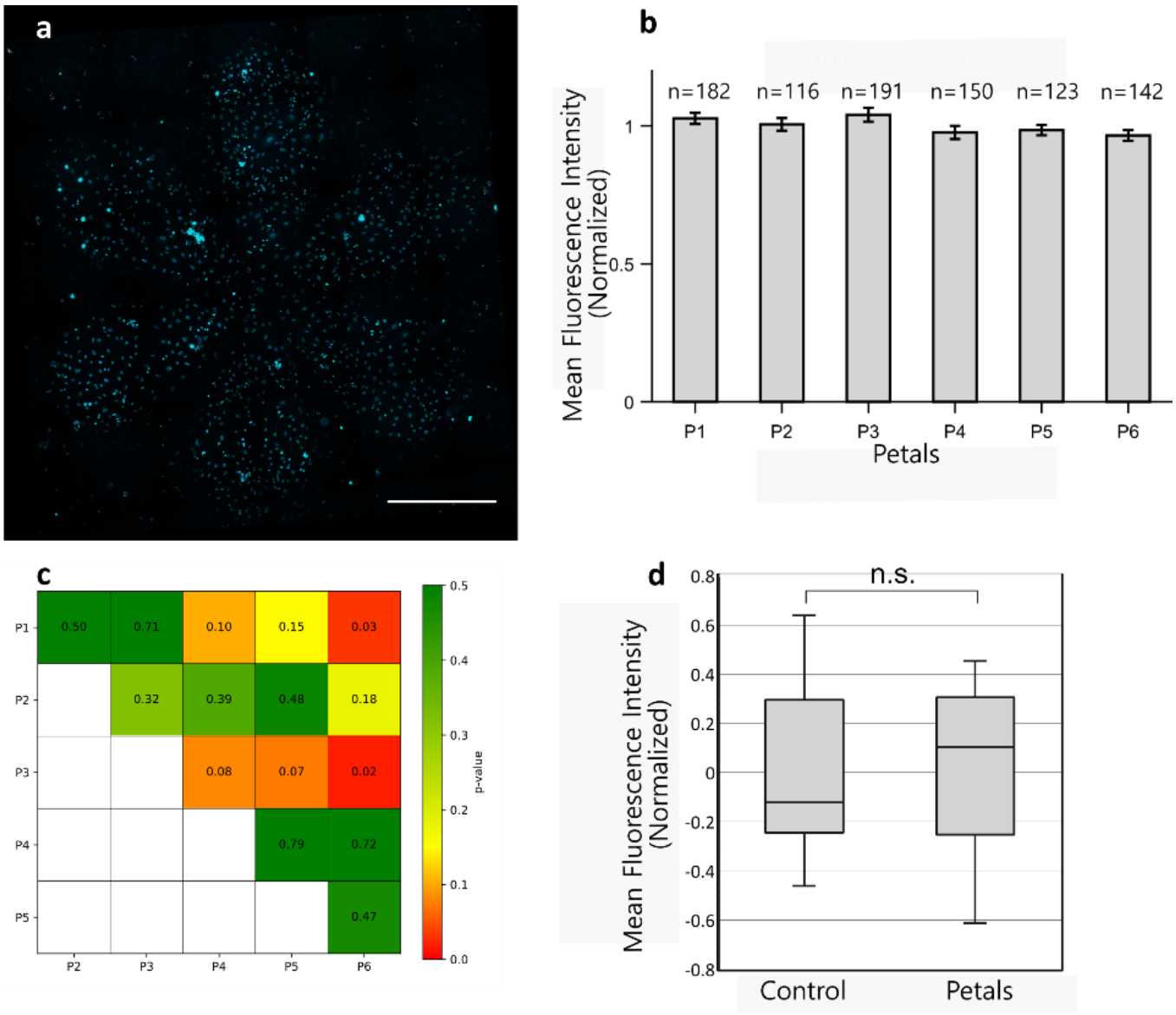


*Fig S3 - Spatial resolution and inter-petal dosage following DNA staining by Hoechst 22358. (a) Fluorescent micrograph of cells stained with Hoechst 22358 for 20 minutes with the microfluidic display. $Q_{inj}$ = 0.4 µL/s and α = 1.3 Scale bar = 500 µm. (b) Mean fluorescence intensity for each petal calculated from the micrograph in (a). The number of cells per petal is shown above the bars. Error bars represent the standard error. (c) Inter-petal comparison of normalized mean fluorescence intensity. ns = non statistically significative difference, s = statistically significative difference ($p_{value}$<0.05). (d) Normalized fluorescence Tukey distributions of intensity for manually stained cells (Control) and cells stained with Hoeschst 223358 for 20 minutes with the microfluidic display (Petals) (3 experiments, 6 petals per experiment).*

# III. Cell viability

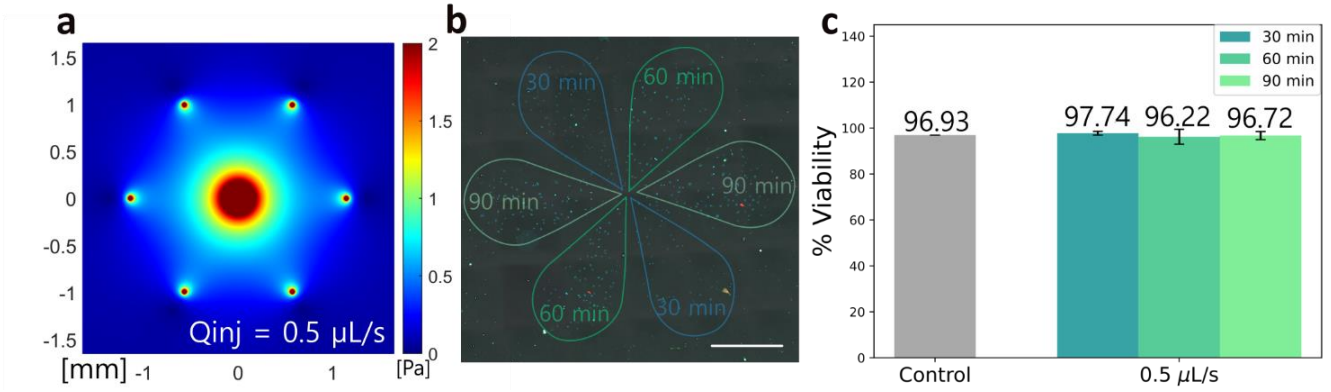


*Fig S4 - Viability results for $Q_{inj}$ =0.5 µL/s, α=0.5. (a) Shear stress map. The area under 1 Pa is greater than the 0.4 mm² threshold established to contain 100 cells at 50% confluency. (b) Exposition time of C2C12 cells to continuous flow. Injection media contains Hoechst 33258. Red nuclei represent dead cells marked with PI. Green cells show apoptotic cells marked by AnnexinV-FITC. Scale bar = 500 µm. (c) Cell viability according to exposition duration to a continuous flow. Control cells were placed in the same incubator, without exposition to the microfluidic display. Error bars represent standard error from petal duplicates.*

# IV. Fluorescence intensity quantification – mCherry signal

To ensure that the mCherry background signal in the nuclei minimally impaired our Hes1 mRNA quantification, we calculated the z-score of the Hes1 signal compared to the nuclear background as mentioned in the main text (Table S2). We also asked whether the nuclei FI had an impact on the number of dots we counted by plotting the mean nuclear FI against the counted mRNAs per cell (Fig S5). We find a $R^2$ coefficient of 0.3159, which indicates a poor correlation between the mCherry signal intensity and the number of mRNA dots. We thus show that the number of dots detected is independent of the nuclear intensity. Finally, Fig S6 shows a fluorescence micrograph of the Hes1 mRNA channel and a snapshot from the Matlab dot-counting algorithm showing the detected mRNA

*Table S2 – Characterization of the contrast between the fluorescence intensity (FI) of the mRNA dots and FI of the nuclei caused by the mcherry reporter in the Hes1 imaging channel. The values are normalized to the maximal intensity in the nuclei.*

| Mean dot FI | Mean nuclei FI | Mean standard deviation in the cell nuclei | Signal to noise ratio |
|---|---|---|---|
| 0.70 | 0.45 | 0.1 | 2.5 |

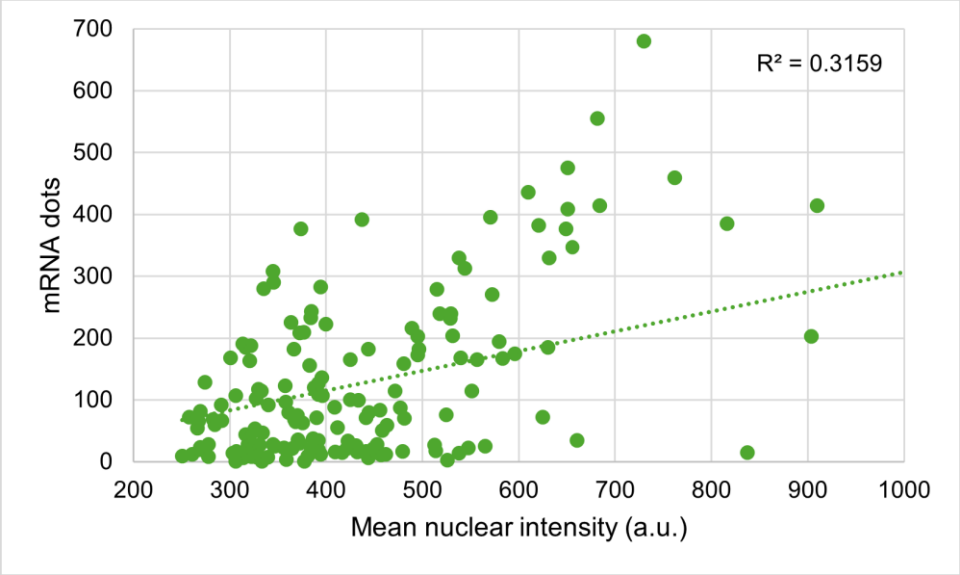


*Fig S5 – Mean nuclear intensity and its corresponding number of mRNA dots. Individual dots correspond to single cells.*

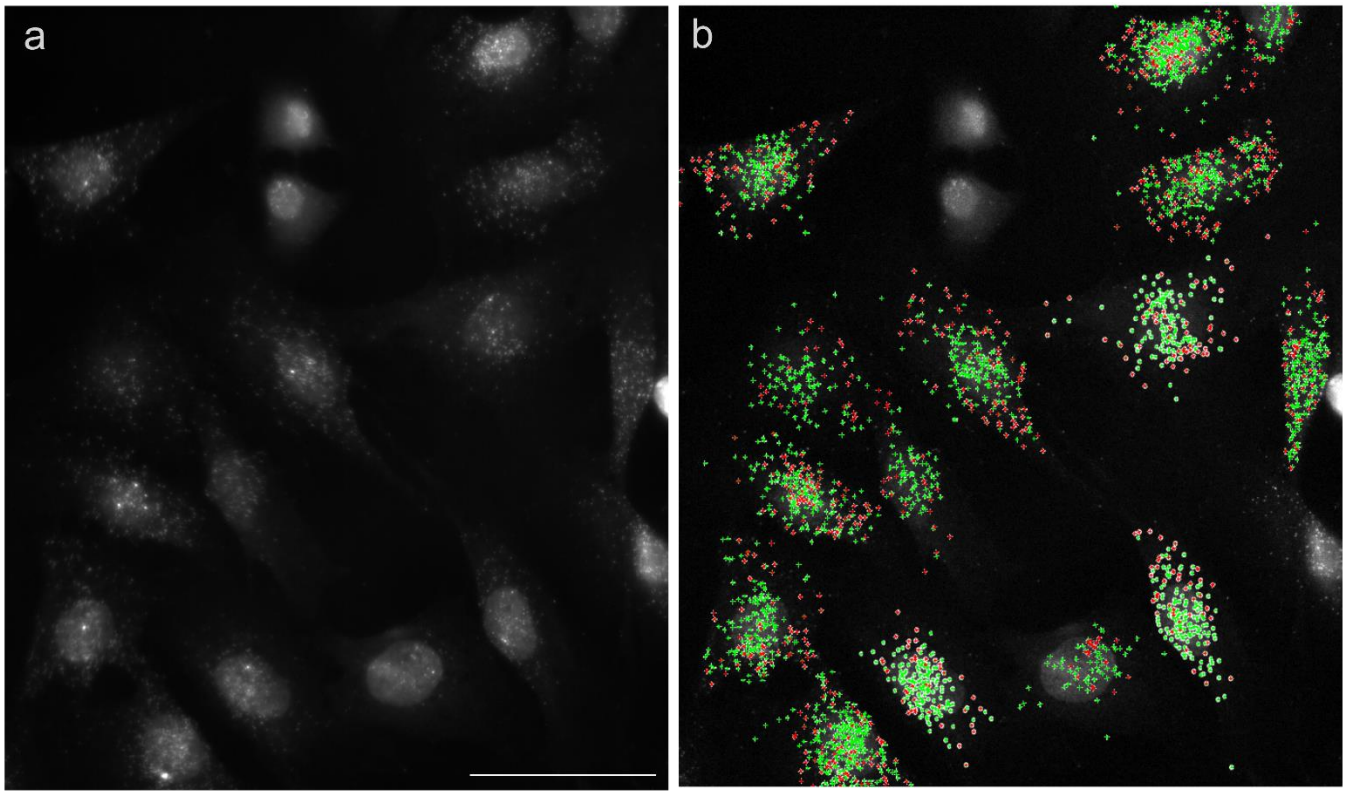


*Fig S6 - Results from the dotCounting algorithm. (a) Grayscale example fluorescence micrograph. The cells showed here were exposed to a 1h DAPT-removal pulse (image taken from the data used to make Fig 4c in the main text, condition P3). Scale bar is 50 µm (b) Corresponding mRNA dots counted by the Matlab algorithm. The red points correspond to mRNA dots which centroids are in the displayed z-stack image. The green points correspond to mRNA dots that were counted in another z-stack slice.*

# V. Notch dynamics validation

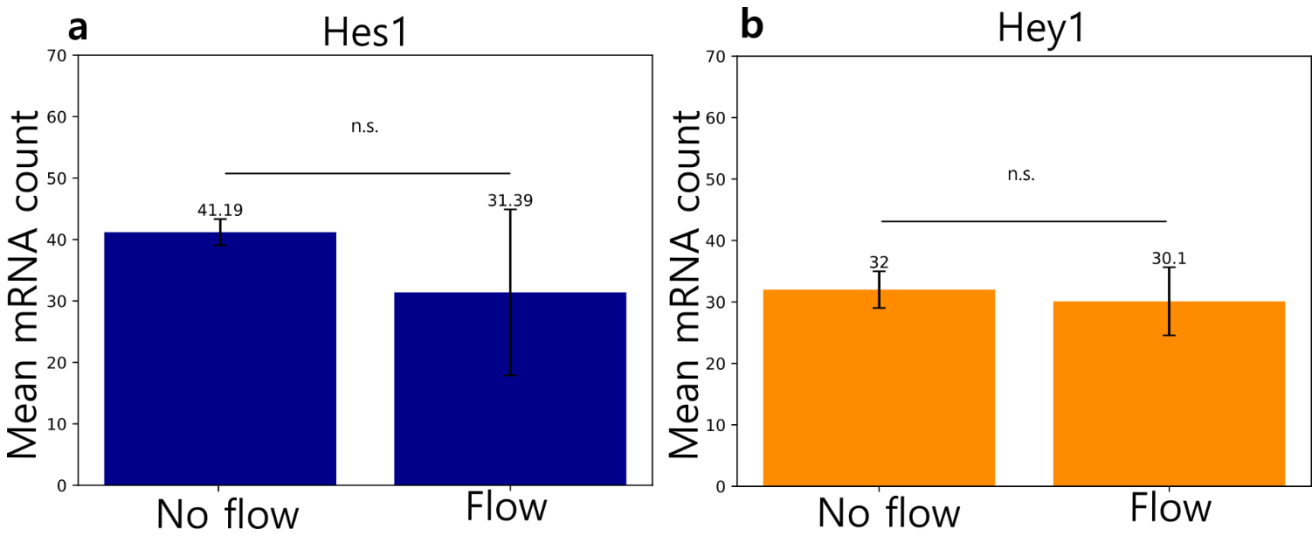


*Fig S7 - Comparison of mRNA expression for cells in 10 µM DAPT in culture (No Flow) and cells exposed to a continuous flow of 10 µM DAPT with the microfluidic display (Flow). (a) Hes1 mRNA count and (b) Hey1 mRNA count.*

# VI. Gene response across experiments

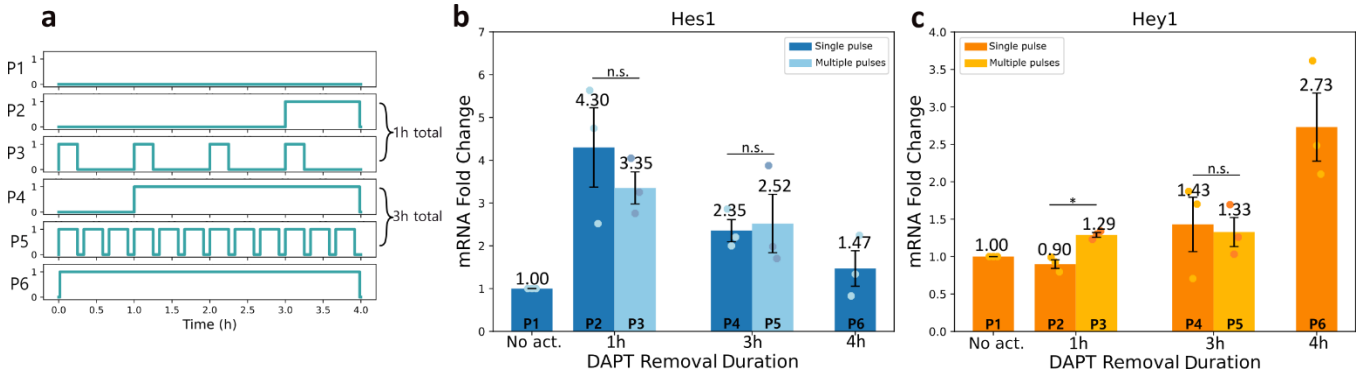


*Fig S8 – Single-pulse and multiple-pulses Notch1 activation of C2C12-ΔECD cells in a single well. (a) Media without DAPT was delivered with a microfluidic display in either a single pulse (in P2 and P4) or in 15-minute pulses (P3, P5 and P6). The total dose of media without DAPT remained constant from P2 to P3 and P4 to P5. (b)(c) Resulting Hes1 and Hey1 expression over the No act. (P1) condition. N=3, Error bars represent SEM, *p<0.05.*

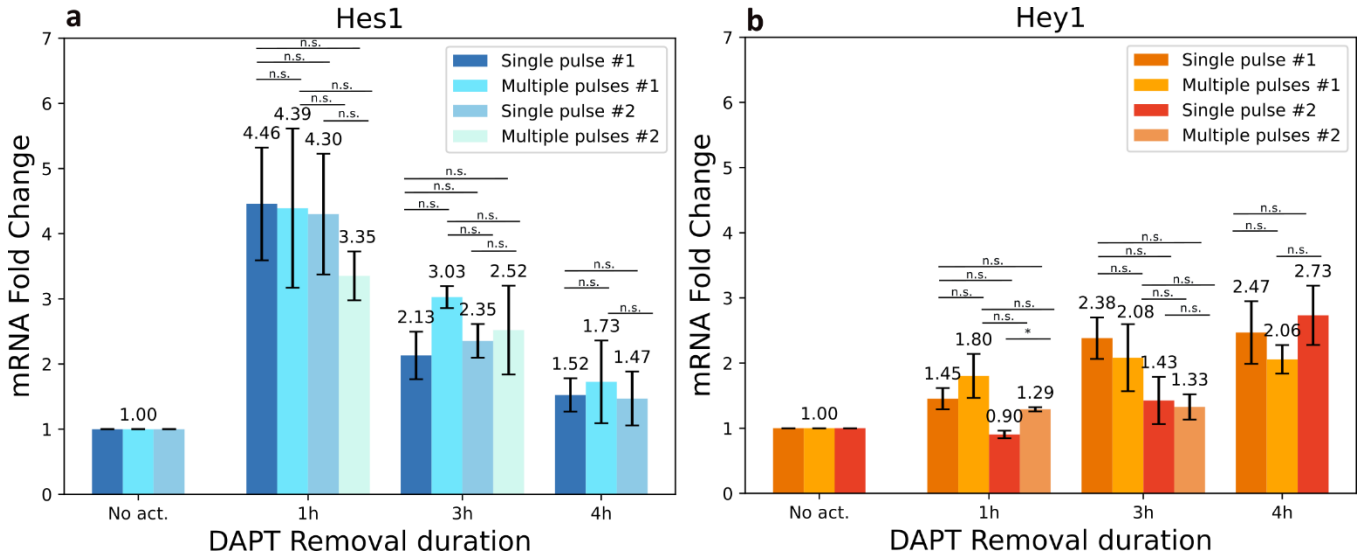


*Fig S9 – Comparison of mRNA expression across experiments. The considered experiments consist of the single pulse experiment (Fig 4 in the main text), multiple pulses experiment (Fig 5 in the main text), and dual single and multiple pulses experiment (Fig S8). Comparisons are done within groups exposed to the same total DAPT removal duration, i.e. with the same total duty cycle. (a) Hes1 comparisons and (b) Hey1 comparisons. One-way ANOVA, post-hoc HSD, *p<0.05.*

# VII. Notch Dynamics Mathematical Model in C2C12-ΔN1ECD cells.

## A. Model description

*Table S3. List of variable definitions*

| Variable | Initial Value | Description |
|---|---|---|
| DAPT | 1 or 0 | Inhibitor of NICD cleaving. When DAPT=0, NICD is released. |
| NICD | 0 | Proportion of cleaved NICD that may bind promoters |
| hes1n | $hes1n_{eq}$ | Hes1 non-mature (nuclear) mRNA. |
| hes1m | $hes1m_{eq}$ | Hes1 mature (cytoplasmic) mRNA. |
| Hes1p | $Hes1p_{eq}$ | Hes1 protein. |
| hey1n | $hey1n_{eq}$ | Hey1 non-mature (nuclear) mRNA. |
| hey1m | $hey1m_{eq}$ | Hey1 mature (cytoplasmic) mRNA. |
| Hey1p | $Hey1p_{eq}$ | Hey1 protein. |

Assumptions and approximations:

1. Maturing time of both hes1 and hey1 mRNA is similar.
2. DAPT is removed (DAPT = 0) or added (DAPT=1) from the system, and acts instantly, i.e. allows NICD release when removed or completely inhibits $\gamma$-secretase when added.
3. NICD instantly binds the RBJ$\kappa$ complex and recruit the co-factors necessary to initiate transcription. For simplicity, NICD is used alone to represent Notch1-mediated transcription.
4. There is a non-depletable source of NICD. Therefore, while DAPT = 1, NICD levels remain maximal.
5. Hill coefficients for both Hes1 and Hey1 mediated transcription repression is 4 (see table S3). Indeed, stability analysis from the Hes1 autorepression loop model developed by Bernard and colleagues showed that $hill \geq 4$.[3]
6. One mRNA dot in the HCR-FISH images corresponds to one mRNA.

$$NICD\ (t) = \begin{cases} 1 \mid DAPT = 0 \\ NICD(t-1) * e^{-\frac{1}{\tau_{NICD}}} \mid DAPT = 1 \end{cases} \quad (1)$$

$$\frac{\partial hes1n}{\partial t} = -\frac{hes1n}{\tau_{delay}} + \frac{k_A * NICD + k_B}{1 + \left(\frac{Hes1p}{K_{Hes1\rightarrow hes1}}\right)^{hill} + \left(\frac{Hey1p}{K_{Hey1p\rightarrow hes1}}\right)^{hill}} \quad (2)$$

$$\frac{\partial hes1m}{\partial t} = -\frac{hes1m}{\tau_{hes1}} + \frac{hes1n}{\tau_{delay}} \quad (3)$$

$$\frac{\partial Hes1}{\partial t} = -\frac{Hes1}{\tau_{Hes1}} + k_{hes1} hes1m \quad (4)$$

$$\frac{\partial hey1n}{\partial t} = -\frac{hey1n}{\tau_{delay}} + \frac{k_c * NICD + k_D}{1 + \left(\frac{Hes1p}{K_{Hes1\rightarrow hey1}}\right)^{hill} + \left(\frac{Hey1p}{K_{Hey1\rightarrow hey1}}\right)^{hill}} \quad (5)$$

$$\frac{\partial hey1m}{\partial t} = -\frac{hey1m}{\tau_{hey1}} + \frac{hey1n}{\tau_{delay}} \quad (6)$$

$$\frac{\partial Hey1}{\partial t} = -\frac{Hey1}{\tau_{Hey1}} + k_{hey1} hey1m \quad (7)$$

*Table S4. List of parameters and their values*

| Parameters | Value | Description | Units | Ref |
|---|---|---|---|---|
| $\tau_{NICD}$ | $\frac{30}{\ln(2)} \approx 43.3$ | Time constant related to the half life of NICD | $min$ | [4–6] |
| $\tau_{delay}$ | $\frac{15}{\ln(2)} \approx 21.6$ | Time constant related to mRNA maturing and exporting time | $min$ | [7,8]* |
| $hill$ | 4 | Hill coefficient, cooperativity | - | [3,9,10] |
| $\tau_{hes1}$ | $\frac{24}{\ln(2)} \approx 34.6$ | Time constant related to the half life of hes1 mRNA | $min$ | [11,12] |
| $\tau_{Hes1}$ | $\frac{22}{\ln(2)} \approx 31.7$ | Time constant related to the half life of Hes1 proteins | $min$ | [11] |
| $k_{hes1}$ | 1 | Protein synthesis rate for Hes1 protein length (282 aa) (Uniprot number: P35428) | $min^{-1}$ | [13]* |
| $K_{Hes1\rightarrow hes1}$ | $5 * Hes1_{eq} \approx 3500$ | Threshold at which half of Hes1 proteins are bound to hes1 promoter | $proteins$ | Estimate |
| $K_{Hey1\rightarrow hes1}$ | $Hey1_{eq} \approx 7100$ | Threshold at which half of Hey1 proteins are bound to hes1 promoter | $proteins$ | Estimate |
| $\tau_{hey1}$ | $\frac{140}{\ln(2)} \approx 202.0$ | Time constant related to the half life of hey1 mRNA | $min$ | [12] |
| $K_{Hes1\rightarrow hey1}$ | $5 * Hes1_{eq} \approx 3500$ | Threshold at which half of Hes1 proteins are bound to hey1 promoter | $proteins$ | Estimate |
| $K_{Hey1\rightarrow hey1}$ | $2 * Hey1_{eq}$ | Threshold at which half of Hey1 proteins are bound to hey1 promoter | $proteins$ | Estimate |
| $k_{hey1}$ | 1 | Protein synthesis rate for Hey1 protein length (299 aa) (Uniprot number: Q9WV93) | $min^{-1}$ | [13]* |
| $\tau_{Hey1}$ | $\frac{140}{\ln(2)} \approx 202.0$ | Time constant related to the half life of Hey1 protein, | $min$ | Estimated from Hey1 mRNA half-life. |

*Values taken from Bionumbers (BNID: 105622, 105650, 104598).

### B. mRNA and protein concentrations at equilibrium, without NICD

To assess concentrations $hes1n_{eq}, hes1m_{eq}, hey1n_{eq}, hey1m_{eq}$ , we used HCR-FISH mRNA dots from our data for cells continuously exposed to DAPT, to approximate the number mRNAs when Notch1 is not

activated. Representative control samples are presented at Fig S10. The mean of mRNA dots per cell for all our Notch activation experiments (9 in total) were used:

$$hes1tot_{eq} = hes1n_{eq} + hes1m_{eq} \approx mean([43\ 44\ 84\ 58\ 16\ 19\ 15\ 18\ 31]) \approx \ 36\ mRNA$$

$$hey1tot_{eq} = hey1n_{eq} + hey1m_{eq} \approx mean([45\ 54\ 75\ 40\ 21\ 29\ 31\ 18\ 39]) \approx \ 39\ \ mRNA$$

To find $hes1n_{eq}$ and $hes1m_{eq}$, we consider:

$$hes1n_{eq} = \frac{\left(hes1m_{eq} * \tau_{Delay}\right)}{\tau_{hes1}} \qquad 11$$

We find:

$$hes1m_{eq} = \frac{hes1tot_{eq}}{1 + \frac{\tau_{delay}}{\tau_{hes1}}} \approx 22\ mRNA$$

and $hes1n_{eq} \approx 14\ mRNA$. Similarly, for hey1, we find $hey1m_{eq} \approx 35\ mRNA$ and $hey1n_{eq} \approx 4\ mRNA$.

To find $Hes1p_{eq}$ and $Hey1p_{eq}$, simply:

$$Hes1p_{eq} = k_{hes1} * \tau_{Hes1} * hes1m_{eq} \approx 750\ proteins$$

$$Hey1p_{eq} = k_{hey1} * \tau_{Hey1} * hey1m_{eq} \approx 6770\ proteins$$

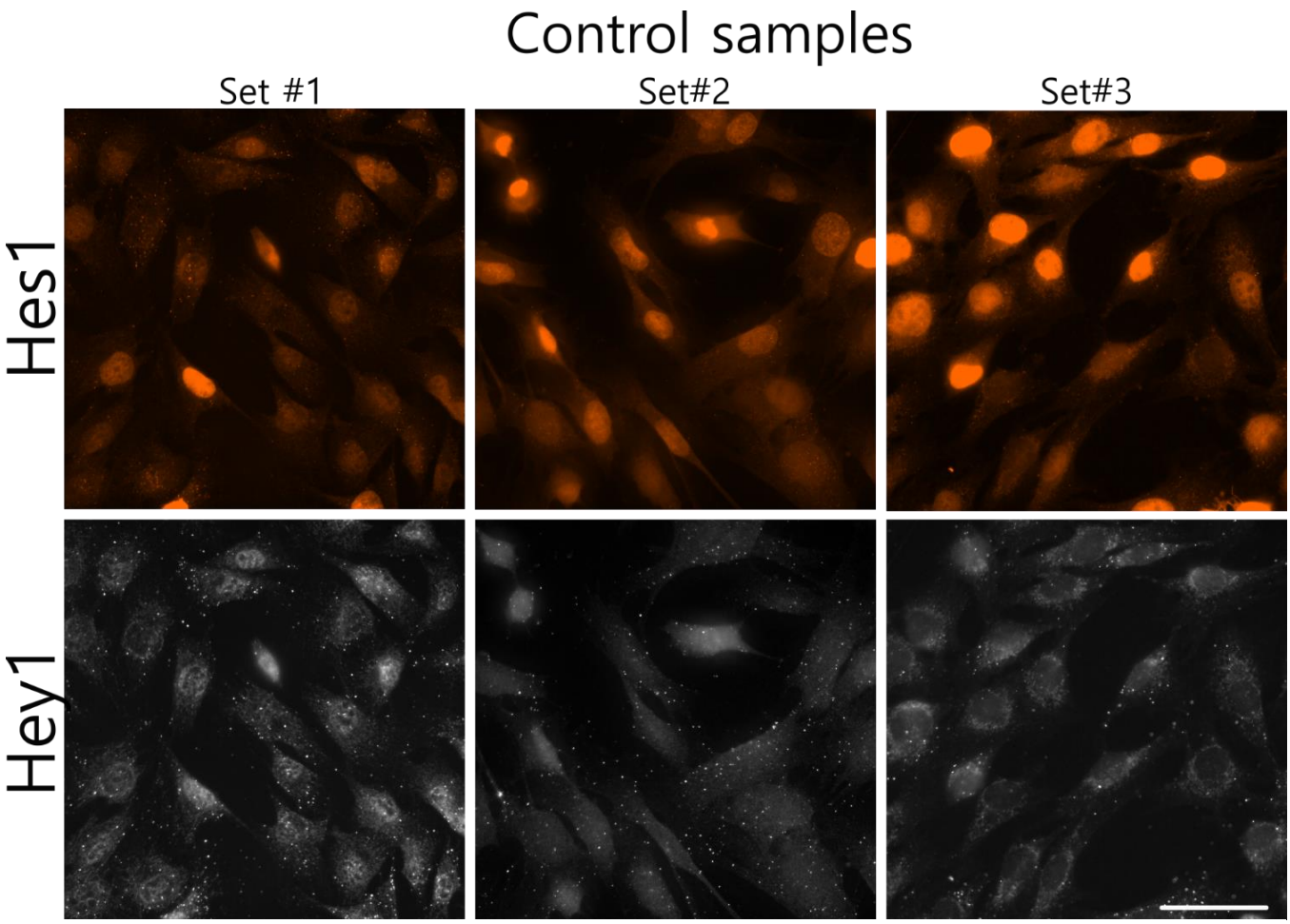


*Fig S10 - Fluorescence micrographs of C2C12-ΔECD cells continuously exposed to 10 µM DAPT, inhibiting NICD release. These samples correspond to the control condition, i.e. cells under the first petal (P1), for each Notch activation experiment. Samples from set #1, #2, and #3 are issued respectively from one of the continuous activation experiments (see Fig4 in the main text), one of the pulsatile activation experiments (see Fig 5 in the main text) and one of the dual continuous and pulsatile activation experiments (see Fig S8). Scale bar = 50 µm.*

**Transcription rates**

To calculate transcription rates related to our model ($k_A, k_B, k_C, k_D$), let us consider the basal hes1 transcription rate, at equilibrium, without NICD. At equilibrium, with $NICD = 0$, $Eq\ (2)$ becomes:

$$\frac{\partial hes1n}{\partial t} = 0 = -\frac{hes1n}{\tau_{delay}} + \frac{k_B}{1 + \left(\frac{Hes1p}{K_{Hes1\to hes1}}\right)^{hill} + \left(\frac{Hey1p}{K_{Hey1p\to hes1}}\right)^{hill}}$$

$$k_B = \frac{hes1n_{eq}}{\tau_{delay}}\left(1 + \left(\frac{Hes1p}{K_{Hes1\to hes1}}\right)^{hill} + \left(\frac{Hey1p}{K_{Hey1p\to hes1}}\right)^{hill}\right)$$

For parameters described in Table 2, $k_B \approx 1.29\ mRNA/min$.

Similarly, for hey1, at equilibrium with NICD = 0, eq (7) becomes:

$$\frac{\partial hey1n}{\partial t} = 0 = k_D - \frac{hey1n_{eq}}{\tau_{delay}}$$

and we find $k_D = \frac{hey1n_{eq}}{\tau_{delay}}\left(1 + \left(\frac{Hes1p}{K_{Hes1\to hey1}}\right)^{hill} + \left(\frac{Hey1p}{K_{Hey1\to hey1}}\right)^{hill}\right) \approx 0.175\, mRNA/min.$

*Table S5 - Transcription rates (mRNA/min)*

| Rate | Description | Value |
|---|---|---|
| $k_A$ | hes1 transcription in presence of NICD. | $5k_B$ |
| $k_B$ | Basal hes1 transcription rate | 1.29 |
| $k_C$ | hey1 transcription rate in presence of NICD. | $3k_D$ |
| $k_D$ | Basal hey1 transcription rate | 0.18 |

## C. Results – Pulsatile activation

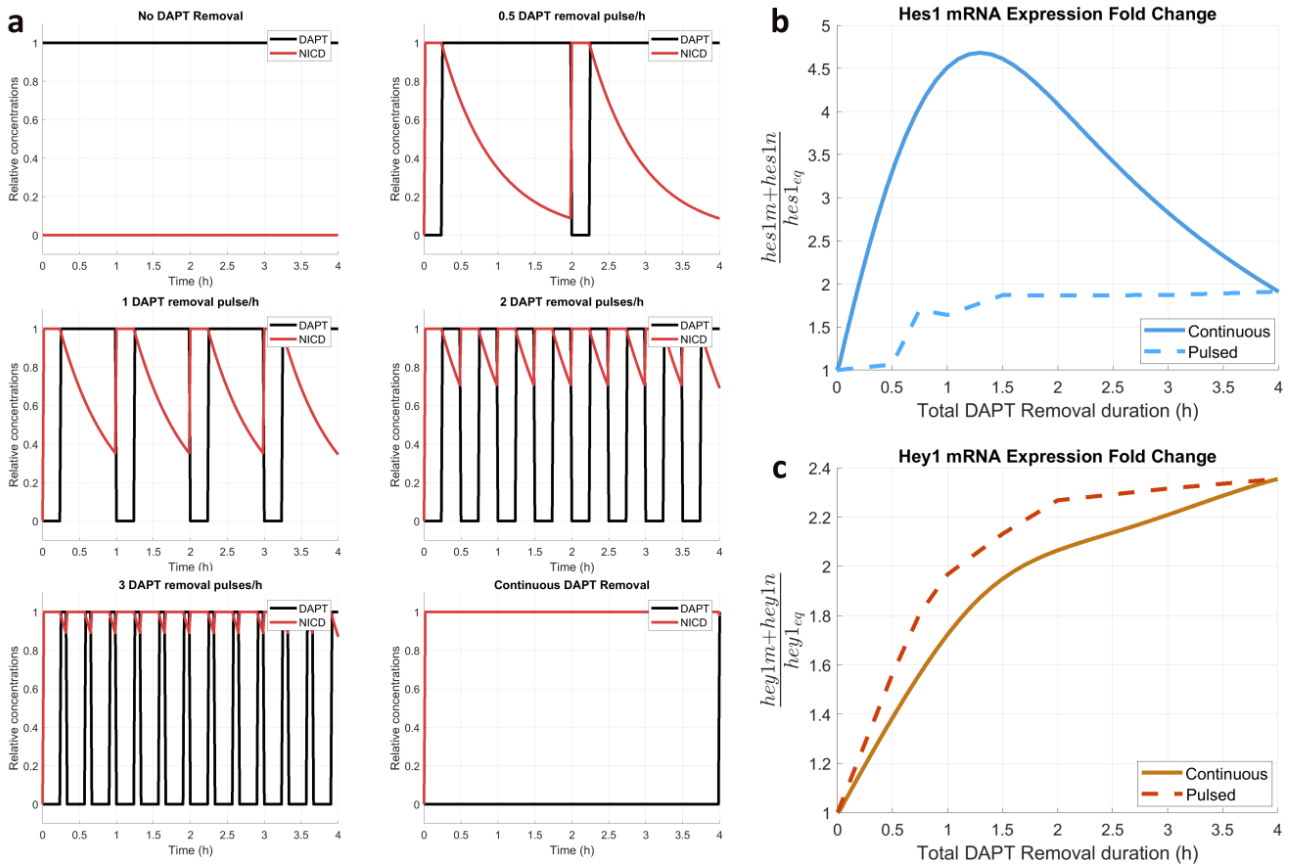


*Fig S11 Comparison of continuous and pulsatile Notch activation with the mathematical model. (a) Examples of different input signals. DAPT removal saturates NICD levels. (b) Hes1 mRNA expression fold change following continuous DAPT removal or pulsatile DAPT removal. (c) Hes1 mRNA expression fold change following continuous DAPT removal or pulsatile DAPT removal.*

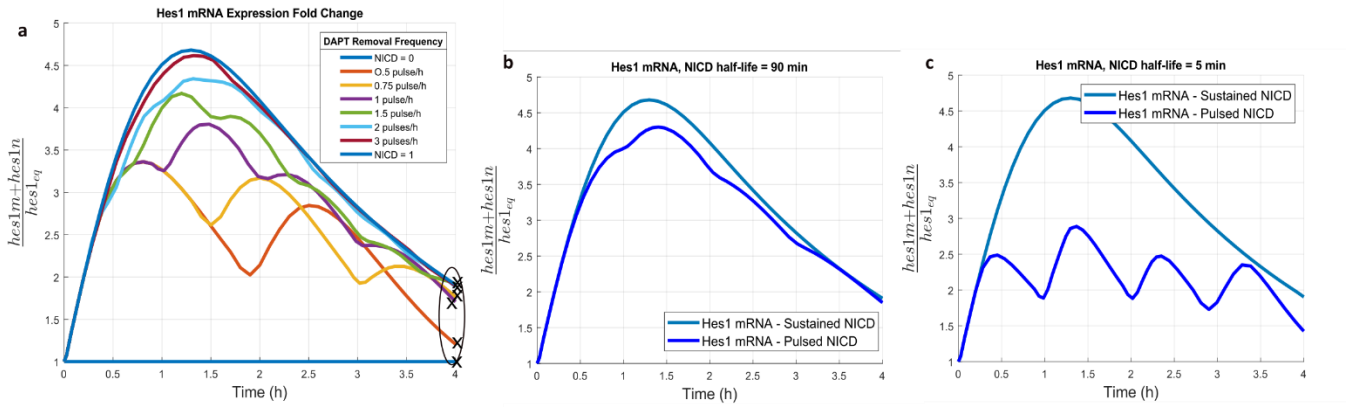


*Fig S12 – Modeled Hes1 mRNA expression characterization following pulsatile DAPT removal and NICD release. (a) Hes1 expression fold change across time over 4h due to different 15-minutes DAPT removal frequency pulses. The circled points represent the values used to plot the dotted line at Fig S11b. NICD half-life is 30 minutes. (b) Hes1 mRNA expression for sustained NICD release, and one 15-minute DAPT removal pulse per hour. NICD half-life is 90 minutes. (c) Hes1 mRNA expression for sustained NICD release, and one 15-minute DAPT removal pulse per hour. NICD half-life is 5 minutes.*

# VIII. References


1 M. Safavieh, M. A. Qasaimeh, A. Vakil, D. Juncker and T. Gervais, *Sci. Rep.*, 2015, **5**, 11943.

2 P.-A. Goyette, É. Boulais, F. Normandeau, G. Laberge, D. Juncker and T. Gervais, *Nat. Commun.*, 2019, **10**, 1781.

3 S. Bernard, B. Čajavec, L. Pujo-Menjouet, M. C. Mackey and H. Herzel, *Philos. Trans. R. Soc. Math. Phys. Eng. Sci.*, 2006, **364**, 1155–1170.

4 C. J. Fryer, J. B. White and K. A. Jones, *Mol. Cell*, 2004, **16**, 509–520.

5 B. E. Housden, A. Q. Fu, A. Krejci, F. Bernard, B. Fischer, S. Tavaré, S. Russell and S. J. Bray, *PLOS Genet.*, 2013, **9**, e1003162.

6 Z. Luo, L. Mu, Y. Zheng, W. Shen, J. Li, L. Xu, B. Zhong, Y. Liu and Y. Zhou, *J. Mol. Cell Biol.*, 2020, **12**, 345–358.

7 H. C. Schröder, U. Friese, M. Bachmann, T. Zaubitzer and W. E. G. Müller, *Eur. J. Biochem.*, 1989, **181**, 149–158.

8 A. Mor, S. Suliman, R. Ben-Yishay, S. Yunger, Y. Brody and Y. Shav-Tal, *Nat. Cell Biol.*, 2010, **12**, 543–552.

9 M. h Jensen, K. Sneppen and G. Tiana, *FEBS Lett.*, 2003, **541**, 176–177.

10 N. A. M. Monk, *Curr. Biol.*, 2003, **13**, 1409–1413.

11 H. Hirata, S. Yoshiura, T. Ohtsuka, Y. Bessho, T. Harada, K. Yoshikawa and R. Kageyama, *Science*, 2002, **298**, 840–843.

12 Y. Harada, M. Yamada, I. Imayoshi, R. Kageyama, Y. Suzuki, T. Kuniya, S. Furutachi, D. Kawaguchi and Y. Gotoh, *Nat. Commun.*, 2021, **12**, 6562.

13 S.-O. Olofsson, K. Boström, P. Carlsson, J. Borén, M. Wettesten, G. Bjursell, O. Wiklund and G. Bondjers, *Am. Heart J.*, 1987, **113**, 446–452.